



Cite this: *Chem. Commun.*, 2022, 58, 6482

Received 15th March 2022,  
Accepted 27th April 2022

DOI: 10.1039/d2cc01476a

rsc.li/chemcomm

# Bis[cyclic (alkyl)(amino)carbene] isomers: Stable *trans*-bis(CAAC) versus facile olefin formation for *cis*-bis(CAAC)†

Braulio M. Puerta Lombardi,<sup>‡a</sup> Ethan R. Pezoulas,<sup>‡a</sup> Roope A. Suvinen,<sup>id b</sup> Alexander Harrison,<sup>a</sup> Zachary S. Dubrawski,<sup>id a</sup> Benjamin S. Gelfand,<sup>id a</sup> Heikki M. Tuononen<sup>id \*b</sup> and Roland Roesler<sup>id \*a</sup>

Isomeric bis(aldiminium) salts with a 1,4-cyclohexylene framework were synthesized. The first isolable bis(CAAC) was prepared from the *trans*-stereoisomer and its ditopic ligand competency was proven by conversion to iridium(i) and rhodium(i) complexes. Upon deprotonation, the *cis*-isomer yielded an electron rich olefin via a classic, proton-catalyzed pathway. The C=C bond formation from the desired *cis*-bis(CAAC) was shown to be thermodynamically very favorable and to involve a small activation barrier. Compounds that can be described as insertion products of the *cis*-bis(CAAC) into the E–H bonds of NH<sub>3</sub>, CH<sub>3</sub>CN and H<sub>2</sub>O were also identified.

First reported in 2005,<sup>1</sup> cyclic (alkyl)(amino)carbenes (CAACs) have been rapidly incorporated into the main-group and organometallic ligand toolkit. Their exceptional  $\sigma$ -donating and  $\pi$ -accepting abilities led to the isolation of a flurry of compounds of fundamental and applied interest.<sup>2</sup> Prominent examples include homoleptic late transition metal compounds in low oxidation states,<sup>3</sup> main-group and organoradical spin carriers,<sup>4</sup> elements in unusual oxidation states,<sup>5</sup> and high-performing transition metal catalysts.<sup>6</sup> The growing library of accessible CAACs is facilitating steric and electronic profile tuning of their complexes for tailored applications.<sup>7–9</sup> Along with the much used five-membered Me<sub>2</sub>CAAC,<sup>1</sup> CyCAACs,<sup>1</sup> and AdCAAC,<sup>10</sup> other examples include CAACs incorporating imine or phosphine pendant arms,<sup>11</sup> six-membered CAAC-6,<sup>12</sup> and bicyclic BiCAACs<sup>13</sup> (Chart 1). The steady expansion of the CAAC library was facilitated by the straightforward access to the respective aldiminium-salt precursors starting from ubiquitous building blocks, via an elegant protonation-cyclization-hydroiminium sequence reported by Bertrand.<sup>14</sup>

Despite the growing library of CAAC ligands and the tremendous success of bis(NHC)<sup>15</sup> (NHC = *N*-heterocyclic carbene) and bisphosphine analogs,<sup>16</sup> no bis(CAAC) has been reported to date. We reasoned that this notable absence could be remedied in few synthetic steps, by formally derivatizing CyCAAC,<sup>1</sup> which was shown to be a competent ligand. The cyclohexyl scaffold could be used to build two desirable bis(CAAC)s: A bidentate *cis*-stereoisomer and a ditopic *trans*-stereoisomer (Chart 1). Our investigations targeting these derivatives will be reported herein.

Aldiminium precursors **3a** and **4a** were obtained in gram quantities via standard CAAC-building protocols,<sup>14</sup> adapted to accommodate the second CAAC moiety (Scheme 1). A commercially available isomeric mixture of cyclohexane-1,4-dimethanols was converted to cyclohexyl-1,4-dicarboxaldehydes and, following condensation with DippNH<sub>2</sub> (Dipp = 2,6-diisopropylphenyl), pure *trans*-diimine **1a** could be isolated in 29% overall yield. Double deprotonation of this precursor with *n*-butyllithium followed by reaction of the resulting aza-allyl anion with 3-bromo-2-methylpropene generated *cis*- and *trans*-**2a**, which were isolated as a mixture.

Layering benzene solutions of this mixture with acetonitrile resulted in selective crystallization of *trans*-**2a** as large colorless blocks in 10% yield. This compound was then subjected to the hydroiminium procedure, leading to dialdiminium tetrafluoroborate salt **3a**. *cis*-Dialdiminium tetrafluoroborate **4a** was more conveniently obtained by carrying on the hydroiminium

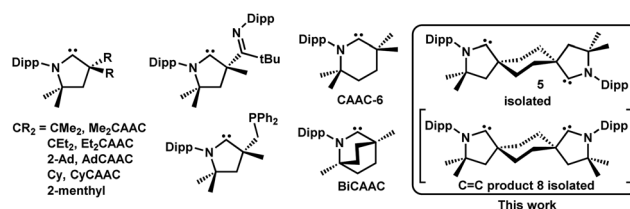


Chart 1 Selected examples of CAACs.

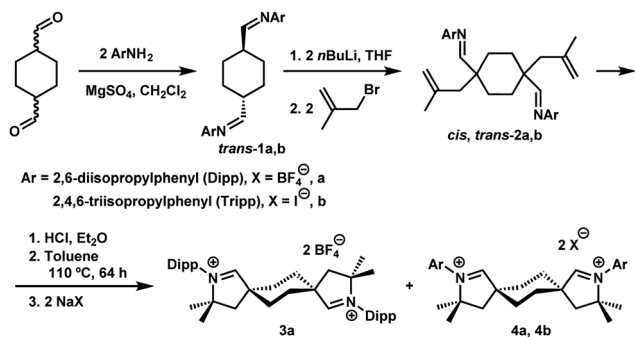
<sup>a</sup> Department of Chemistry, University of Calgary, 2500 University Drive NW, Calgary, AB, T2N 1N4, Canada. E-mail: roesler@ucalgary.ca

<sup>b</sup> Department of Chemistry, Nanoscience Centre, University of Jyväskylä, P.O. Box 35, FI-40014 Jyväskylä, Finland. E-mail: heikki.m.tuononen@jyu.fi

† Electronic supplementary information (ESI) available. CCDC 2131007–2131017. For ESI and crystallographic data in CIF or other electronic format see DOI: <https://doi.org/10.1039/d2cc01476a>

‡ These authors contributed equally to this work.

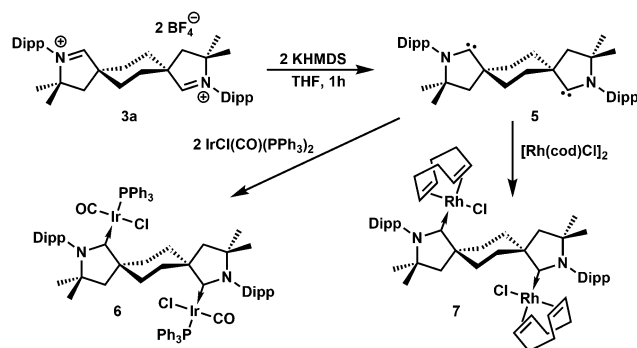




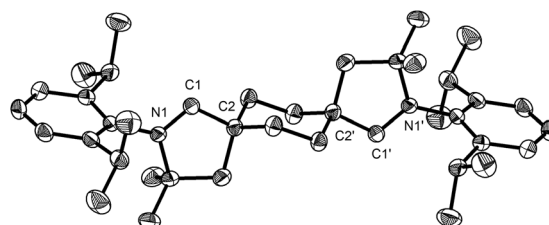
**Scheme 1** Succession of reactions leading to the synthesis of bis(CAAC) precursors **3a** and **4a,b**.

reaction with a mixture of *cis*- and *trans*-**2a**. Extraction of the product mixture with  $\text{CHCl}_3$  and recrystallization by layering  $\text{CH}_2\text{Cl}_2$  solutions with hexanes yielded **4a** in 67% yield. The configuration of the aldiminium fragments was readily assessed by  $^1\text{H}$  NMR, based on coupling patterns for the cyclohexylene linker protons (in  $\text{CD}_2\text{Cl}_2$ , **3a** exhibits two doublet resonances at 1.93 and 2.65 ppm and **4a** features a pair of multiplets at 2.20 and 2.52 ppm), and confirmed by single-crystal X-ray diffraction (Fig. 1).

Addition of two equivalents of potassium hexamethyldisilazide (KHMDs) to *trans*-aldiminium salt **3a** in THF produced the expected dicarbene **5** (Scheme 2 and Fig. 2), displaying a characteristic  $^{13}\text{C}$  NMR resonance corresponding to the carbene carbons at 315.2 ppm in  $\text{C}_6\text{D}_6$ . Under an inert atmosphere, **5** could be handled at room-temperature and no decomposition was observed by  $^1\text{H}$  NMR after storing the solid at  $-40^\circ\text{C}$  for a month. The ditopic nature of **5** was probed *via* reaction with  $\text{IrCl}(\text{CO})(\text{PPh}_3)_2$  or  $[\text{Rh}(\text{cod})\text{Cl}]_2$  in benzene, which yielded complexes **6** (Fig. 3) and **7** (Fig. S67, ESI $^\dagger$ ), respectively, as yellow, crystalline precipitates. The four ligands in **6** adopt a



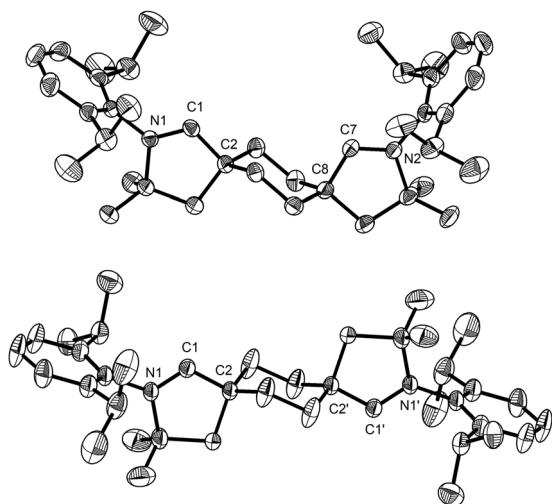
**Scheme 2** Synthesis of free dicarbene **5** and its metal complexes **6** and **7**.



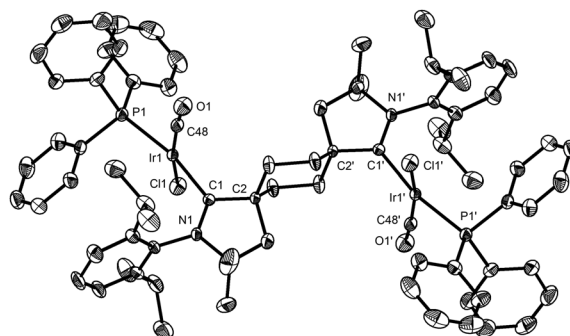
**Fig. 2** Solid-state structure of **5** with 50% probability thermal ellipsoids and hydrogen atoms omitted for clarity. Selected bond lengths [Å] and angles [°]: N1–C1 1.3065(16), C1–C2 1.5232(17); N1–C1–C2 105.92(10).

square planar coordination geometry at iridium, with  $\text{PPh}_3$  *trans* to the carbene, as previously observed in analogous  $\text{IrCl}(\text{CO})(\text{NHC})(\text{PPh}_3)$  complexes.<sup>17</sup> The spectral signature of **6** ( $\delta_{\text{carbene}}$  255 ppm,  $\delta_{\text{CO}}$  174 ppm,  $\delta_{\text{P}}$  22 ppm,  $\nu_{\text{CO}}$  1950  $\text{cm}^{-1}$ ) is also similar to that of  $\text{IrCl}(\text{CO})(\text{NHC})(\text{PPh}_3)$  ( $\delta_{\text{carbene}}$  178 ppm,  $\delta_{\text{CO}}$  171 ppm,  $\delta_{\text{P}}$  25 ppm,  $\nu_{\text{CO}}$  1945  $\text{cm}^{-1}$ ).<sup>17</sup>

Addition of two equivalents of  $\text{Et}_3\text{N}$ ,  $\text{iPr}_2\text{NEt}$ ,  $\text{LiHMDS}$ ,  $\text{LDA}$ ,  $\text{MeLi}$  or  $\text{Me}_3\text{SiCH}_2\text{Li}$  to a suspension **4a** in THF of led to intractable mixtures. When lithium-2,2,6,6-tetramethylpiperidide ( $\text{LiTMP}$ ) was employed, an elimination reaction took place, regenerating *cis*-**2a**. A similar behavior was reported by Bertrand for CAAC-6.<sup>12</sup> Immediately upon addition of two equivalents of KHMDs to **4a** at  $-78^\circ\text{C}$ , (Fig. S55 and S56, ESI $^\dagger$ ), a singlet resonance was detected at

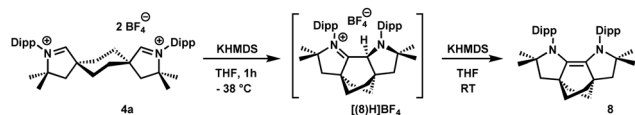


**Fig. 1** Solid-state structures of the dications in **3a** (top) and **4a** (bottom) with 50% probability ellipsoids and hydrogen atoms omitted for clarity. Selected bond lengths [Å] and angles [°]: **3a**: C1–N1 1.272(4), C1–C2 1.491(4); N1–C1–C2 114.7(2); **4a**: C1–N1 1.275(2), C1–C2 1.482(3); N1–C1–C2 114.76(17).



**Fig. 3** Solid-state structure of **6** with 50% probability thermal ellipsoids and hydrogen atoms omitted for clarity. Selected bond lengths [Å] and angles [°]: Ir1–C1 2.035(3), Ir1–P1 2.3111(8), O1–C48 1.100(3), C1–Ir1–P1 168.68(7), C48–Ir1–Cl1 168.69(9), N1–C1–C2 109.3(2).



Scheme 3 Synthesis of **8** via  $[(8)H]BF_4$ .

318.0 ppm by  $^{13}C$  NMR, suggesting the formation of a CAAC. It rapidly disappeared upon warming to  $-38\text{ }^{\circ}C$  with concurrent emergence of a new set of resonances suggestive of a less symmetric compound. In the  $^1H$  NMR spectrum, a singlet at 5.08 ppm, within the range observed for protonated NHC-CAAC dimers (4.90–5.32 ppm in  $CD_3CN$ ; 4.58, 4.72 ppm in  $CDCl_3$ ),<sup>19</sup> was assigned to the protonated olefin intermediate  $[(8)H]BF_4$  (Scheme 3). Ultimately, warming up the mixture to room temperature led to the formation of a higher-symmetry compound, confirmed *via* X-ray crystallography to be olefin **8** (Fig. S68, ESI<sup>†</sup>); whole-molecule disorder precluded a detailed discussion of bonding parameters. Similar electron-rich olefins were recently reported by Sarkar.<sup>20</sup> Solutions of **8** in toluene were stable up to  $110\text{ }^{\circ}C$  and the solid could be handled in air. The substantial steric crowding in **8** forces the nitrogen atoms to become pyramidalized (sum of nitrogen bond angles  $351.4(4)^{\circ}$ ). Furthermore, two methyl groups within the Dipp fragments are forced into close proximity to the opposing aryl ring, giving rise to a strongly shielded  $^1H$  NMR resonance at  $-0.02$  ppm.

DFT studies showed that, upon single deprotonation of **4a** to a free mono-CAAC, the cyclohexane backbone readily changes conformation from chair to twist boat ( $\Delta G_{c\rightarrow tb}^{\ddagger} = 24\text{ kJ mol}^{-1}$ , Fig. S72, ESI<sup>†</sup>). A second conformational change from twist boat to boat, accompanied by the formation of a C–C bond to give  $[8(H)]^+$ , is similarly facile ( $\Delta G_{tb\rightarrow b}^{\ddagger} = 12\text{ kJ mol}^{-1}$ ). The two-step transformation is overall exergonic ( $\Delta G = -72\text{ kJ mol}^{-1}$ ) and expected to take place rapidly even at  $-38\text{ }^{\circ}C$  due to the associated small energy barriers. The calculated  $^1H$  NMR chemical shifts of  $[8(H)]^+$  are in good agreement with the experimental values, with a characteristic singlet at 5.91 ppm *vs.* 5.08 ppm observed experimentally for the protonated olefin. A hypothetical *cis*-bis(CAAC) resulting from double deprotonation of **4a** gave a potential energy surface similar to single deprotonation, with greater energy barriers for conformational changes of the cyclohexane ring ( $\Delta G_{c\rightarrow tb}^{\ddagger} = 52$  and  $\Delta G_{tb\rightarrow b}^{\ddagger} = 40\text{ kJ mol}^{-1}$ , Fig. S73, ESI<sup>†</sup>). This likely stems from the increased repulsion associated with two carbon atoms with lone pairs. The formation of **8** from the *cis*-bis(CAAC) is overall highly exergonic ( $\Delta G = -262\text{ kJ mol}^{-1}$ ) as a C=C double bond is formed between the two carbenic carbon atoms.

The calculations support the intermediacy of  $[8(H)]BF_4$  en route from **4a** to **8**. Furthermore, even though double deprotonation of **4a** could take place prior to conformational changes, the energy barriers associated with the cyclohexane ring flip are minor. This suggests that the *cis*-bis(CAAC) species obtained *via* double deprotonation of **4a** is not isolable under any conditions. While these results might initially seem surprising, they become less so upon comparison with data calculated for the

dimerization of  $Me_2CAAC$ , which show  $\Delta G_{dimer} = -75$  and  $-99\text{ kJ mol}^{-1}$  for *cis* and *trans* product geometries, respectively. Thus, dimerization of two CAACs is always thermodynamically favored but generally kinetically blocked by very high activation barriers ( $\Delta G_{cis}^{\ddagger} = 189$  and  $\Delta G_{trans}^{\ddagger} = 188\text{ kJ mol}^{-1}$ ) that arise in large part from the entropic penalty of dimerization ( $-T\Delta S = 81\text{ kJ mol}^{-1}$ ). No such penalty exists when the two CAAC moieties are part of the same molecule, which supports the facile formation of **8**.

Cyclic voltammetry of **8** in THF revealed two reversible redox waves ( $E_{1/2} = -0.32$  and  $0.49$  *vs.*  $Fe/Fe^+$ , Fig. S59, ESI<sup>†</sup>), corresponding to the oxidation of **8** to its radical cation and further to the dication, respectively. Both oxidations are anodically-shifted in comparison to the values reported by Sarkar,<sup>20</sup> potentially due to the inductive effect of the *N*-aryl substituent in **8** leading to a less electron rich system. The  $C_2$ -symmetric radical cation was isolated as purple tetrafluoroborate salt **9** following the oxidation of **8** with  $[Ph_3C][BF_4]$ . It was characterized by EPR (Fig. S60, ESI<sup>†</sup>) and its structure was confirmed by X-ray crystallography (Fig. 4).

Attempting to destabilize the electron rich olefin **8** in favor of a free *cis*-bis(CAAC), the Dipp substituents in **4a** were replaced with Tripp (2,4,6-triisopropylphenyl) (Scheme 1). However, deprotonation of **4b** also led to C=C bond formation and this chemistry will not be detailed here. We then turned our attention to complex formation directly from **4a**, by employing metal reagents featuring Brønsted-basic ligands (Scheme 4). The reaction of NHC salt precursors with  $Cu_2O$  or  $Ag_2O$  to yield the corresponding metal complexes has been extensively explored.<sup>21</sup> Extrapolation of this method to CAACs is less common,<sup>22</sup> arguably due to the weaker acidity of aldiminium-CAAC salts. Heating an acetonitrile solution of **4a** with  $Cu_2O$  over several days in an NMR tube resulted in crystallization of colorless blocks that were identified as ether **12** by single-crystal X-ray diffraction (Fig. S71, ESI<sup>†</sup>). The structure is reminiscent of the  $(Me_2CAACH)_2O$  ether obtained as a side-product while preparing  $(Me_2CAAC)_2Ge$ .<sup>23</sup> Refluxing **4a** and  $Fe(HMDS)_2$  in acetonitrile led to crystallization of **11** (Fig. S65, ESI<sup>†</sup>). The presence of  $(Me_3Si)_2NH$  in the NMR of the product mixture suggests that deprotonation may indeed take place. However, scaling up the reaction led to the isolation of **10** instead (Fig. S70, ESI<sup>†</sup>). The origin of the nitrogen atom is presumably  $(Me_3Si)_2NH$ , a byproduct from the reaction of  $Fe(HMDS)_2$

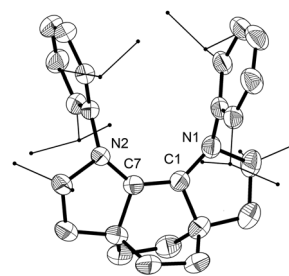
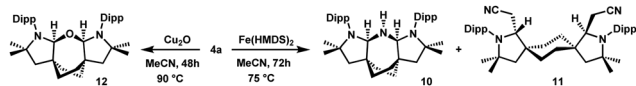


Fig. 4 Solid-state structure of the cation in **9** with 50% thermal ellipsoids and hydrogen atoms omitted for clarity. Selected bond lengths (Å) and angles ( $^{\circ}$ ): C1–C7 1.409(3), C1–N1 1.357(3), C7–N2 1.360(3).







Scheme 4 Reactivity of **4a** towards transition metal complexes with Brønsted-basic ligands.

and **4a**. Attempted complex formation using  $\text{Ca}(\text{HMDS})_2$ ,  $\text{Mg}(\text{SiTMS}_3)_2$ ,  $\text{Pd}(\text{OAc})_2$ , or  $[\text{PtMe}_2(\mu\text{-SMe}_2)]_2$  gave intractable mixtures.

In conclusion, two isomeric CAAC-aldiminium salts **3a** and **4a**, derived from the same parent aldehydes, were synthesized on multi-gram scale. *trans*-Stereoisomer **3a** was doubly deprotonated to yield the first isolable bis(CAAC) **5**, which proved to easily form dinuclear metal complexes, as exemplified by iridium complex **6** and rhodium complex **7**. Upon double deprotonation with  $\text{KHMDs}$ , *cis*-stereoisomer **4a** formed the electron-rich olefin **8**. Experimental and computational studies suggest the process follows the classic Lewis-acid catalyzed NHC dimerization pathway. DFT calculations showed that the intramolecular C=C bond formation in a free *cis*-bis(CAAC) derived from **4a** is highly exergonic ( $-262 \text{ kJ mol}^{-1}$  vs.  $-75 \text{ kJ mol}^{-1}$  for *cis*-dimerization of  $\text{Me}_2\text{CAAC}$ ) and involves, for entropic reasons, a small activation barrier that can be lowered even more by proton catalysis. Reaction of **4a** with metal complexes featuring Brønsted-basic ligands led to the identification of **10**, **11**, and **12**, which can be described as insertion products of a bis(CAAC) into the N-H, C-H and O-H bonds of  $\text{NH}_3$ ,  $\text{CH}_3\text{CN}$  and  $\text{H}_2\text{O}$ , respectively. Whether their formation involves a free CAAC intermediate that has been observed at low-temperature by NMR, as described for mono(CAAC)s,<sup>24</sup> or the transient formation of metal complexes, remains to be investigated. 17 years after the first report of a CAAC ligand, our study adds the first bis(CAAC) ligand to the organometallic toolkit.

Financial support was provided by the Universities of Calgary and Jyväskylä, as well as the Natural Sciences and Engineering Research Council of Canada (NSERC) in the form of Discovery Grant #2019-07195 to R. R. The project received funding from the European Research Council under the EU's Horizon 2020 programme (grant #772510 to H. M. T.). A. H. and Z. S. D. acknowledge funding from the Canada First Research Excellence Fund (CFREF). Computational resources were provided by the Finnish Grid and Cloud Infrastructure (persistent identifier urn:nbn:fi:research-infras-2016072533).

## Conflicts of interest

There are no conflicts to declare.

## References

- V. Lavallo, Y. Canac, C. Präsang, B. Donnadieu and G. Bertrand, *Angew. Chem., Int. Ed.*, 2005, **44**, 5705–5709.
- M. Soleilhavoup and G. Bertrand, *Acc. Chem. Res.*, 2015, **48**, 256–266; M. Melaimi, R. Jazzar, M. Soleilhavoup and G. Bertrand, *Angew. Chem., Int. Ed.*, 2017, **56**, 10046–10068; V. Nesterov, D. Reiter, P. Bag, P. Frisch, R. Holzner, A. Porzelt and S. Inoue, *Chem. Rev.*, 2018, **118**, 9678–9842; S. K. Kushvaha, A. Mishra, H. W. Roesky and K. C. Mondal, *Chem. – Asian J.*, 2022, e2021013.
- S. Roy, K. C. Mondal and H. W. Roesky, *Acc. Chem. Res.*, 2016, **49**, 357–369.
- M. M. Hansmann, M. Melaimi, D. Munz and G. Bertrand, *J. Am. Chem. Soc.*, 2018, **140**, 2546–2554; M. M. Hansmann, M. Melaimi and G. Bertrand, *J. Am. Chem. Soc.*, 2018, **140**, 2206–2213; T. Ullrich, P. Pinter, J. Messelberger, P. Haines, R. Kaur, M. M. Hansmann, D. Munz and D. M. Guldi, *Angew. Chem., Int. Ed.*, 2020, **59**, 7906–7914.
- M. Arrowsmith, H. Braunschweig, M. A. Celik, T. Dellermann, R. D. Dewhurst, W. C. Ewing, K. Hammond, T. Kramer, I. Krummenacher, J. Mies, K. Radacki and J. K. Schuster, *Nat. Chem.*, 2016, **8**, 890–894; W. Lu, Y. Li and R. Kinjo, *J. Am. Chem. Soc.*, 2019, **141**, 5164–5168.
- M. P. Wiesenfeldt, Z. Nairoukh, W. Li and F. Glorius, *Science*, 2017, **357**, 908–912; J. Morvan, M. Mauduit, G. Bertrand and R. Jazzar, *ACS Catal.*, 2021, **11**, 1714–1748.
- Y. Gao, S. Yazdani, A. Kendrick IV, G. P. Junor, T. Kang, D. B. Grotjahn, G. Bertrand, R. Jazzar and K. M. Engle, *Angew. Chem., Int. Ed.*, 2021, **60**, 19871–19878.
- D. Pichon, M. Soleilhavoup, J. Morvan, G. P. Junor, T. Vives, C. Crevisy, V. Lavallo, J. M. Campagne, M. Mauduit, R. Jazzar and G. Bertrand, *Chem. Sci.*, 2019, **10**, 7807–7811.
- J. Morvan, F. Vermersch, Z. Zhang, L. Falivene, T. Vives, V. Dorcet, T. Roisnel, C. Crevisy, L. Cavallo, N. Vanthuyne, G. Bertrand, R. Jazzar and M. Mauduit, *J. Am. Chem. Soc.*, 2020, **142**(47), 19895–19901.
- V. Lavallo, G. D. Frey, S. Kousar, B. Donnadieu and G. Bertrand, *Proc. Natl. Acad. Sci. U. S. A.*, 2007, **104**, 13569–13573.
- J. Chu, D. Munz, R. Jazzar, M. Melaimi and G. Bertrand, *J. Am. Chem. Soc.*, 2016, **138**, 7884–7887.
- C. M. Weinstein, G. P. Junor, D. R. Tolentino, R. Jazzar, M. Melaimi and G. Bertrand, *J. Am. Chem. Soc.*, 2018, **140**, 9255–9260.
- E. Tomás-Mendivil, M. M. Hansmann, C. M. Weinstein, R. Jazzar, M. Melaimi and G. Bertrand, *J. Am. Chem. Soc.*, 2017, **139**, 7753–7756.
- R. Jazzar, R. D. Dewhurst, J.-B. Bourg, B. Donnadieu, Y. Canac and G. Bertrand, *Angew. Chem., Int. Ed.*, 2007, **46**, 2899–2902; R. Jazzar, J.-B. Bourg, R. D. Dewhurst, B. Donnadieu and G. Bertrand, *J. Org. Chem.*, 2007, **72**, 3492–3499.
- M. Poyatos, J. A. Mata and E. Peris, *Chem. Rev.*, 2009, **109**, 3677–3707; M. Poyatos and E. Peris, *Dalton Trans.*, 2021, **50**, 12748–12763.
- In *Phosphorus(III) Ligands in Homogeneous Catalysis: Design and Synthesis*, ed. P. C. J. Kamer and P. W. N. M. van Leeuwen, Wiley, New York, 2012; A. L. Clevenger, R. M. Stolley, J. Aderibigbe and J. Louie, *Chem. Rev.*, 2020, **120**, 6124–6196.
- C.-F. Fu, Y.-H. Chang, Y.-H. Liu, S.-M. Peng, C. J. Elsevier, J.-T. Chen and S.-T. Liu, *Dalton Trans.*, 2009, 6991–6998.
- D. Munz, J. Chu, M. Melaimi and G. Bertrand, *Angew. Chem., Int. Ed.*, 2016, **55**, 12886–12890; J. Messelberger, A. Grünwald, S. J. Goodner, F. Zeilinger, P. Pinter, M. E. Miehl, F. W. Heinemann, M. M. Hansmann and D. Munz, *Chem. Sci.*, 2020, **11**, 4138–4149.
- D. Mandal, R. Dolai, R. Kumar, S. Suhr, N. Chrysochos, P. Kalita, R. S. Narayanan, G. Rajaraman, C. Schulzke, B. Sarkar, V. Chandrasekhar and A. Jana, *J. Org. Chem.*, 2019, **84**, 8899–8909.
- M. K. Nayak, S. Suhr, N. Chrysochos, H. Rawat, C. Schulzke, V. Chandrasekhar, B. Sarkar and A. Jana, *Chem. Commun.*, 2021, **57**, 1210–1213.
- I. J. B. Lin and C. S. Vasam, *Coord. Chem. Rev.*, 2007, **251**, 642–670; M. R. L. Furst and C. S. J. Cazin, *Chem. Commun.*, 2010, **46**, 6924.
- Y. D. Bidal, O. Santoro, M. Melaimi, D. B. Cordes, A. M. Z. Slawin, G. Bertrand and C. S. J. Cazin, *Chem. – Eur. J.*, 2016, **22**, 9404–9409.
- Y. Li, K. C. Mondal, H. W. Roesky, H. Zhu, P. Stollberg, R. Herbst-Irmer, D. Stalke and D. M. Andradá, *J. Am. Chem. Soc.*, 2013, **135**, 12422–12428.
- G. D. Frey, V. Lavallo, B. Donnadieu, W. W. Schoeller and G. Bertrand, *Science*, 2007, **316**, 439–441.

